mg05-19

Semivariogram Models Based On Geometric Offsets

Michael J. Pyrcz[1] and Clayton V. Deutsch[2]

Author Coordinates:

[1] Quantitative Stratigraphy, Earth Science R & D, Chevron Energy Technology Company, Houston, TX 77002 USA; e-mail: mjpy@chevron.com

[2] Department of Civil and Environmental Engineering, University of Alberta, Edmonton, AB T6G 2W2 Canada; e-mail: cdeutsch@ualberta.ca

Suggested Running Head: *Geometric Semivariograms*

Corresponding Author: Michael J. Pyrcz
Quantitative Stratigraphy, Earth Science R & D
Chevron Energy Technology Company
Houston, TX 77002

E-mail: mjpy@chevron.com

Phone: 1 832 854 7016

ABSTRACT

Kriging-based geostatistical models require a semivariogram model. Next to the initial decision of stationarity, the choice of an appropriate variogram model is the most important decision in a geostatistical study. Common practice consists of fitting experimental semivariograms with a nested combination of proven models such as the spherical, exponential, and Gaussian models. These models work well in most cases; however, there are some shapes found in practice that are difficult to fit. We introduce a family of semivariogram models that are based on geometric shapes, analogous to the spherical semivariogram, that are known to be conditional negative definite and that provide additional flexibility to fit semivariograms encountered in practice. A methodology to calculate the associated geometric shapes to match semivariograms defined in any number of directions is presented. Greater flexibility is available through the application of these geometric semivariogram models.

Keywords: nested structures, kriging, stochastic simulation, geostatistics

INTRODUCTION

Kriging-based geostatistics is routinely used for estimation and simulation of continuous and categorical geologic properties. The random function paradigm of geostatistics involves three main steps: (**1**) definition of the variable and the stationary domain for the variable $\{Z(\mathbf{u}), \mathbf{u} \in A\}$, which involves the definition of rock types/facies and large scale trends, (**2**) establish a semivariogram model for the variable, $\gamma(\mathbf{h})$, that is valid for all distances and directions found in the domain A, and (**3**) make inferences with kriging and Monte Carlo simulation. The reasonableness of the inferences depends on the first two steps (Pyrcz and others, in press). The expert site-specific decision of a stationary domain is arguably the most important; however, the calculation and fitting of a semivariogram model is also very important. The inference step is largely automatic once the first two steps are taken. This paper is aimed at the second step of establishing a valid semivariogram model. The conventional method of modeling semivariograms by nested structures is reviewed. A suite of geometric semivariograms and a method for constructing new geometries that match custom continuity styles are presented. These geometric semivariogram models allow for greater flexibility in the generation of permissible semivariogram models.

CONVENTIONAL SEMIVARIOGRAM MODELING

The semivariogram characterizes spatial variability of the variable under consideration. Semivariogram models must be conditional negative definite; the covariance counterpart must be positive definite. This mathematical property ensures that the semivariogram is an licit measure of distance and that all resulting variances will be non-negative for all possible configurations of conditioning data (Journel and Huijbregts, 1978, p. 35).

Experimental semivariogram points are calculated in the principal directions allowing for some distance and direction tolerance to find sufficient pairs. The experimental points are fitted with a sum of nested structures:

$$\gamma(h) = \sum_{i=0}^{nst} C_i \Gamma_i(\mathbf{h}) \quad \textbf{(1)}$$

where *nst* is the number of nested structures, $i = 0$ is commonly reserved for the nugget effect. The C_i values are the variance contribution of each nested structure; they must be non-negative. The $\Gamma_i(\mathbf{h})$ functions are valid semivariogram functions defined by a shape (e.g., spherical, exponential, Gaussian), rotation angles to allow the vector $\mathbf{h}$ to be represented in the principal directions of continuity (h_1, h_2, h_3), and range parameters (a_1, a_2, a_3) to account for anisotropy. Standardized distances are calculated with the following equation:

$$h = \sqrt{\left(\frac{h_1}{a_1}\right)^2 + \left(\frac{h_2}{a_2}\right)^2 + \left(\frac{h_3}{a_3}\right)^2} \tag{2}$$

The standardized distance *h* is at the range of correlation in all directions. The standardized shape converts the scalar *h* to a standardized variogram value $\Gamma(\mathbf{h})$.

Semivariogram modeling has relied on fitting known conditional negative definite functions such as spherical, exponential and Gaussian models. Linear combinations of semivariogram models and products of covariance models are also valid functions (Deutsch and Journel, 1998, p. 24). While this provides a workable mechanism for modeling most semivariograms, there are some cases that are not well fit with this framework.

Figure 1 shows an example structure commonly observed in experimental semivariograms that is not easy to fit with the conventional structures.

The application of more flexible semivariogram modeling is inhibited by the difficulty in ensuring conditional negative definiteness. There is a largely unexplored suite of conditional negative definite models known as *geometric semivariograms* that provides additional flexibility. They are genetically guaranteed to be conditional negative definite and therefore avoid the burden of proof required by arbitrary semivariogram functions.

The covariance is related to the semivariogram under second order stationarity:

$$C(\mathbf{h}) = \sigma^2 - \gamma(\mathbf{h}) \tag{3}$$

where $C(\mathbf{h})$ is the covariance and σ^2 is the variance. For ease of interpretation, semivariogram tables are shown as covariance tables since this is the common convention in kriging-based geostatistics, as covariance values provide improved stability in the solution of kriging matrices (Deutsch and Journel, 1998).

GEOMETRIC SEMIVARIOGRAMS

Semivariogram models based on a moving average of a generalized Poisson process is conditional negative definite (Matérn, 1960, p. 28). Geometric semivariograms result from the special case of spatial convolution where the weighting function is reduced to a Dirac function of the form:

$$f(\mathbf{u}) = i_v(\mathbf{u}) = \begin{cases} 1, if & \mathbf{u} \in V \\ 0, if & \mathbf{u} \notin V \end{cases}$$

$$F(\mathbf{u}) = K_v(\mathbf{h}) = \int i_v(\mathbf{u}) \cdot i_v(\mathbf{u}+\mathbf{h}) d\mathbf{u} \quad \textbf{(4)}$$

$$\gamma(\mathbf{h}) = 1 - \frac{K_v(\mathbf{h})}{K_v(0)}$$

This amounts to the volume of intersection $K_v(\mathbf{h})$ of any geometric object, *V*, with itself offset by a lag vector, **h** scaled by the volume of the geometric object, $K_v(0)$. Construction of a geometric semivariogram is illustrated in

Figure 2.

A conditional negative definite model in n-D is valid in any less or equal dimensional space; for example, the spherical semivariogram, based on a 3-D geometry, is valid in 3, 2 and 1 dimensions, a circular semivariogram, based on a 2-D geometry, is valid in 2 and 1 dimensions and the triangular semivariogram, based on a 1-D geometry, is valid only in 1 dimension.

In some cases analytical equations may be available for the volumes of intersection. Numerical integration can always be used for complicated geometric objects. The volume of intersection is calculated as:

$$\gamma(\mathbf{h}) = \underbrace{\sum_{i_z}^{n_z}\sum_{i_y}^{n_y}\sum_{i_x}^{n_x} i(\mathbf{u}_x, \mathbf{u}_y, \mathbf{u}_z)}_{K'_V(0)} - \underbrace{\sum_{i_z}^{n_z}\sum_{i_y}^{n_y}\sum_{i_x}^{n_x} i(\mathbf{u}_x, \mathbf{u}_y, \mathbf{u}_z) \cdot i(\mathbf{u}_x + \mathbf{h}_x, \mathbf{u}_y + \mathbf{h}_y, \mathbf{u}_z + \mathbf{h}_z)}_{K'_V(\mathbf{h})} \quad \textbf{(5)}$$

where $i(\mathbf{u}_x, \mathbf{u}_y, \mathbf{u}_z)$ and $i(\mathbf{u}_x + \mathbf{h}_x, \mathbf{u}_y + \mathbf{h}_y, \mathbf{u}_z + \mathbf{h}_z)$ are indicators set to 1 within the object and 0 if outside the object and $K_V'(0)$ is the discretized volume of the geometry and $K_V'(\mathbf{h})$ is the volume of intersection given the component lag vectors $\mathbf{h}_x, \mathbf{h}_y, \mathbf{h}_z$ of lag vector $\mathbf{h}$. The result is a discrete covariance model for kriging or simulation. This discrete covariance model may be represented as a covariance table that may be loaded directly into kriging or a kriging based simulation algorithm.

Limitations of Geometric Semivariogram Models

Geometric semivariogram models have a some limitations in their form. (**1**) it is not possible to model a semivariogram above the sill variance (see Equation 5). This precludes the modeling of trend and hole effect continuity structures. (**2**) The semivariogram is linear at small lag distance. The linear feature at small lag distances prevents geometric semivariogram models from reproducing high short range continuity as seen with the Gaussian semivariogram model (Deutsch and Journel, 1998). (**3**) The semivariogram model is only known at discrete lag distances, unless the analytical solution is known (i.e. spherical semivariogram model). The geometry and semivariogram table are constructed to match a specific regular grid; therefore, the semivariogram may only be applied to calculate the covariance between points on this grid. These models are suitable for simulation of values on a detailed regular grid, which is increasingly common in geostatistical calculations. The data are assigned to the nearest grid node.

Some Isotropic Geometric Semivariogram Models

Isotropic geometric semivariogram models result from isotropic geometric objects. This is limited to combinations of lines (1-D), circles (2-D), spheres (3-D) and hyperspheres (n-D, n > *3*). These geometric models account for anisotropy by scaling the component vectors [Eq. (2)].

The *spherical semivariogram model* is used frequently. The spherical model is based on the standardized volume of intersection of two spheres separated by a lag vector (**h**) as defined (Serra, 1967).

$$\gamma(\mathbf{h}) = 1 - \frac{volume(\mathbf{h})_{\mathrm{int}}}{volume_{total}} \quad \textbf{(6)}$$

where $volume(\mathbf{h})_{\mathrm{int}}$ is the volume of intersection $volume_{total}$ is the total volume of the geometric object.

A variety of other isotropic geometric semivariogram models may be calculated by hollowing of the geometric object. For example the circle in 2-D may be changed to an annular region or the sphere in 3-D may be changed to a hollowed sphere. The hollowed sphere results in a novel series of conditional negative definite 3-D semivariogram models parameterized by the inner radius (r_1) or fraction of hollowing. A series of *hollowed spherical semivariogram* models are shown in

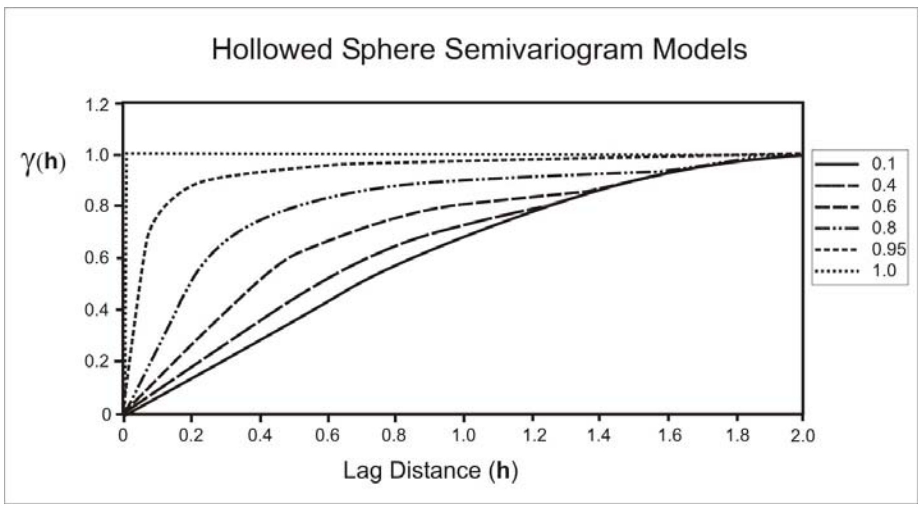

Figure 3.

In the limiting cases this semivariogram is equivalent to the spherical model when r_1 equals 0.0 (the sphere is not hollowed) and approaches the nugget effect as $r_1 \rightarrow r_2$. The difference between the hollowed spherical semivariogram and the spherical semivariogram is equivalent to the volume of intersection lost due to the hollowed inner sphere (Figure 4). An example hollowed sphere (fraction hollowed 0.75) geometry and resulting covariance table are shown in

Figure 5.

Anisotropic Geometric Semivariogram Models

Any geometric shape in any dimension leads to a valid semivariogram model. Slices through an approximated shape of a point bar inclined heterolithic strata (IHS) are shown on the top of

Figure 6. The covariance table is calculated for this object and is shown on the bottom of

Figure 6. This geometric object has resulted in a complicated anisotropic covariance table.

There are a variety of geologic geometries that may be applied to calculate semivariogram models. For example, characteristic geometries of architectural elements from fluvial depositional settings such as lateral accretion, downstream accretion, and channel fills (Miall, 1999, p. 93) may be suitable.

A semivariogram model constructed by an elementary geologic shape does not necessarily mean that the resulting kriged or simulated models will reproduce those shapes. In fact, the underlying indicator semivariogram model for spheres (of proportion $p=1-p_0$) embedded randomly within a matrix is related the spherical variogram, but is not the spherical variogram:

$$\gamma(\mathbf{h}) = p_0\left(1 - p_0^{Sph(\mathbf{h})}\right) \tag{7}$$

Equation 7 could be generalized to account for any geometric variogram in the exponent. Another approach would be to directly calculate the geometry that will match an experimental semivariogram model.

SCULPTED GEOMETRIC SEMIVARIOGRAMS

A method is presented to calculate the geometry to match a target semivariogram in specified directions. An initial geometry is iteratively eroded and dilated. Changes that improve the match between the current geometric model and the target semivariograms are accepted. The resulting geometry may be applied to calculate covariance tables for kriging and simulation.

The Inputs

Custom geometric semivariograms may be constructed to match continuity structures defined in any set of directions. These continuity structures are represented as tables with the target semivariograms and associated lag distance. The practitioner will apply site specific information and professional judgment in assigning these target directional semivariograms. It is anticipated that these models will be fit to at least the principal directions, with additional directions added to further constrain the resulting model.

The Initial Geometry

Initial geometry is coded such that the final model may not have a range greater than the longest identified range nor less than the shortest identified range. The geometry is initialized with an outer ellipsoid of diameter equal to the largest range in all specified directions and an inner ellipsoid of diameter equal to the shortest range. No location outside the outer ellipsoid is allowed to be part of the geometry. Locations inside the inner ellipsoid are not to be taken away from the geometry. The remainder of the space may be switched between 1 and 0 iteratively to improve the reproduction of the target directional semivariograms (

Figure 7). There is no analytical model of anisotropy used for off-diagonal directions, unlike the assumption of an ellipsoidal continuity in the off-diagonal directions in traditional semivariogram models (

Figure 8). Multiple sculpted geometric semivariogram models may be calculated to represent this uncertainty in the off-diagonal directions. If adequate information is available, experimental semivariogram fits in off-diagonal directions may be integrated to further constrain the model.

Zonal anisotropy may be included by setting the initial diameter large relative to the size of the covariance lookup table.

The Iterations and Convergence Criteria

An objective function is applied to characterize mismatch between the target and sculpted geometric semivariogram models. This objective function is shown below:

$$O = \sum_{i=1}^{nDir} \sum_{j=1}^{nLag} \left| \gamma^{geo}(\mathbf{h}_{i,j}) - \gamma^{t}(\mathbf{h}_{i,j}) \right| \qquad \textbf{(8)}$$

where $\gamma^{geo}(\mathbf{h}_{i,j})$ and $\gamma^{t}(\mathbf{h}_{i,j})$ are the current geometric and target semivariogram models for each indicated direction, *i*, and lag, *j*. This objective function weights all lag distances equally. It is common practice to focus on fitting short scale structures, the addition of a weight (such as $1/\mathbf{h}_{i,j}$) would account for this.

The nodes within the modifiable zone (

Figure 7) are visited in order from the outside inwards. This ordering is based on the distance function of initial geometry (Vincent, 1993). This amounts to the assignment of the distance to the nearest periphery of the geometry at all nodes within the geometry. The distance function is sorted in ascending order with pointer arrays permuted.

For each location, the geometry code is switched. The location within the current geometry is eroded ($i\,(\mathbf{u}_i) = 1 \rightarrow 0$) or outside the current geometry dilated ($i\,(\mathbf{u}_i) = 0 \rightarrow 1$). The objective function is updated and if the perturbation reduces the objective function it is accepted. The algorithms proceeds until either a maximum number of iterations are performed or until a specified number of iterations occur without acceptance of a perturbation.

Example Sculpted Semivariogram Models

A large suite of sculpted semivariogram models were calculated. Many unconditional 2-D simulation models were calculated with a variety of input semivariogram parameters (ranges, nugget effects, anisotropies and structure types). Then the experimental semivariograms were calculated for the 0^0, 45^0, 90^0 and 135^0 azimuths. These experimental semivariograms were applied as input for the construction of 2-D sculpted geometric semivariograms. The resulting covariance tables were checked for ill conditioned covariance matrices; all variances were positive (as required by theory) and all kriging weights were reasonable [-1,1].

An example 2-D sculpted geometric semivariogram model is shown in

Figure 9. This example demonstrates the flexibility and some limitations of sculpted semivariogram models. Note that the trend in the input directional variograms is not reproduced since geometric models may not exceed the sill. The zonal anisotropy is not reproduced since the largest range was set to 40 units.

Another example 2-D sculpted geometric semivariogram model is shown in

Figure 10. This model represents a phenomenon with a high nugget effect and a high degree of anisotropy. Note that the nugget effect is reproduced by a lack of contiguity in the geometry and the anisotropy results in anisotropy in the geometry. Another method for incorporating the nugget effect is to model other continuity structures and then add the nugget effect to this discrete model.

SEMIVARIOGRAM MODELING PROCEDURE

The flexible semivariogram modeling is summarized. This methodology requires the following steps: (**1**) assess the continuity of the modeled phenomenon in at least the principal directions, (**2**) construct a geometric object either from characteristic geometries or by the iterative method introduced in this paper with a resolution greater than or equivalent to the resolution of the model to be estimated or simulated, (**3**) calculate a discrete covariance table from this geometry, (**4**) load this covariance table into the kriging or simulation algorithm. These directional models may be regression fits of the experimental semivariogram points, or even hand drawn. The key is to build models that integrate the available geologic information.

CONCLUSIONS

The choice of semivariogram model has a major affect on kriging and kriging-based simulation. These models are commonly modeled as nested combinations of proven models. Geometric semivariogram models provide a suite of conditional negative definite models for improved semivariogram modeling flexibility. A flexible method has been presented for constructing geometries for geometric semivariograms that reproduce spatial continuity identified in principal and additional directions.

The required computer code is straightforward and efficient and is available from the authors. All semivariogram models proposed here are guaranteed to be conditional negative definite; therefore, there are no issues with implementation. Flexible fitting of semivariogram models allows for greater focus on the available experimental semivariogram and geologic information without the limitation imposed with the traditional method of nested structures.

REFERENCES

Deutsch, C.V. and Journel A.G., 1998, GSLIB: geostatistical software library and user's guide 2nd ed.: Oxford University Press, New York, 369 p.

Journel, A.G. and Huijbregts, Ch.J., 1978, Mining geostatistics: Academic Press, New York, 600 p.

Matérn, B., 1960, Spatial variation, volume 36 of lecture notes in statistics 2nd ed.: Springer-Verlag, New York, First edition published by Meddelanden fran Statens Skogsforskningsinstitut, band 49, no. 5, 1960, 151 p.

Miall, A. D., 1996, The geology of fluvial deposits: sedimentary facies, basin analysis and petroleum geology: Springer-Verlag Inc., Berlin, 582 p.

Pyrcz, M.J., Gringarten, E., Frykman, P., and Deutsch, C.V., Representative Input Parameters for Geostatistical Simulation, In: *Stochastic Modeling II: AAPG Computer Applications in Geology, No N*, edited by T.C. Coburn, in press.

Serra, J., 1967, Un critère nouveau de découvertes de structures: le variogramme: Sciences de la Terre, v. 12, p. 275-299.

Vincent, L., 1993, Morphological Algorithms, In: *Mathematical Morphology in Image Processing*, edited by E.R. Dougherty, Marcel Dekker, Inc., New York, p. 255-288.

Figure 1 - An example semivariogram that is not well fit by nested sets of traditional variogram models.

Figure 2 – An example geometric object and the resulting geometric variogram in the horizontal direction. The semivariogram model is anisotropic.

Figure 3 - A series of hollowed sphere semivariogram models. The sphere radius, r2, is set to 1.0 and the radius of the hollowing is varied.

Figure 4 - Volumes v1, v2 and v3 (A, B and C): a traditional spherical variogram model is equal to standardized v1 subtracted from the contribution. The hollowed sphere model is equal to the spherical minus v2 plus v3.

Figure 5 - Center slices through the rasterized geometric object and the resulting covariance table for the hollow spherical model with a hollowed fraction of 0.75.

Figure 6 - Center slices through the raster geometric object and the resulting covariance table for a possible IHS point bar variogram.

Figure 7 – An initial 2-D geometry based on fit semivariograms in three directions. The area outside a circular geometry with a diameter equal to the longest identified range (direction A) is set as permanently outside the geometry. A circular geometry with a diameter equal to the shortest identified range (direction C) is set as permanently inside the geometry. The remainder may be modified iteratively to fit the semivariograms in each identified direction.

Figure 8 – The constraints on sculpted geometric semivariogram models. The major and minor principal directions (directions A and B respectively) and the traditional anisotropy ellipsoid are shown. The sculpted semivariogram model is constrained such that range in the off diagonal directions (such as direction B) may not exceed the range in the major direction or be exceeded by the range in the minor direction. The anisotropy may be expressed in a various forms within this constraint.

Figure 9 – A 2-D geometry and covariance table for a sculpted geometric semivariogram model based on a phenomenon with high continuity. The initial geometry, the target directional models and resulting sculpted geometric semivariogram models in 0^{O}, 45^{O}, 90^{O} and 135^{O} directions are

shown. The longest range of continuity was assigned as 40 units. The target models are experimental semivariograms from unconditional sequential Gaussian simulation.

Figure 10 – A 2-D geometry and covariance table for a sculpted geometric semivariogram model based on a phenomenon with high anisotropy and large nugget effect. The initial geometry, the target directional models and resulting sculpted geometric semivariogram models in 0^{O}, 45^{O}, 90^{O} and 135^{O} directions are shown. The target models are experimental semivariograms from unconditional sequential Gaussian simulation.

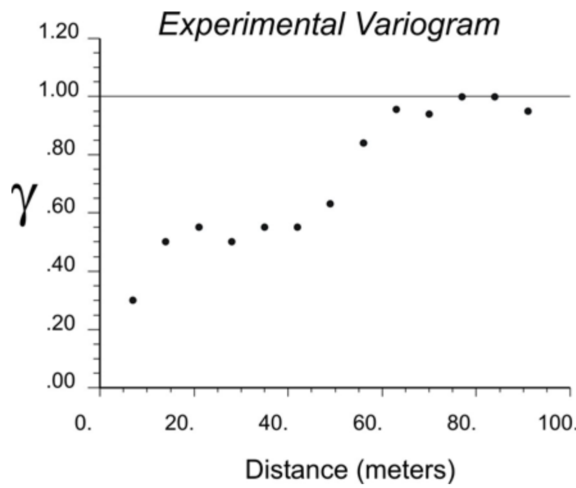
Experimental Variogram
1.20
1.00
.80
γ
.60
.40
.20
.00
0.
20.
40.
60.
80.
100.
Distance (meters)

Figure 1

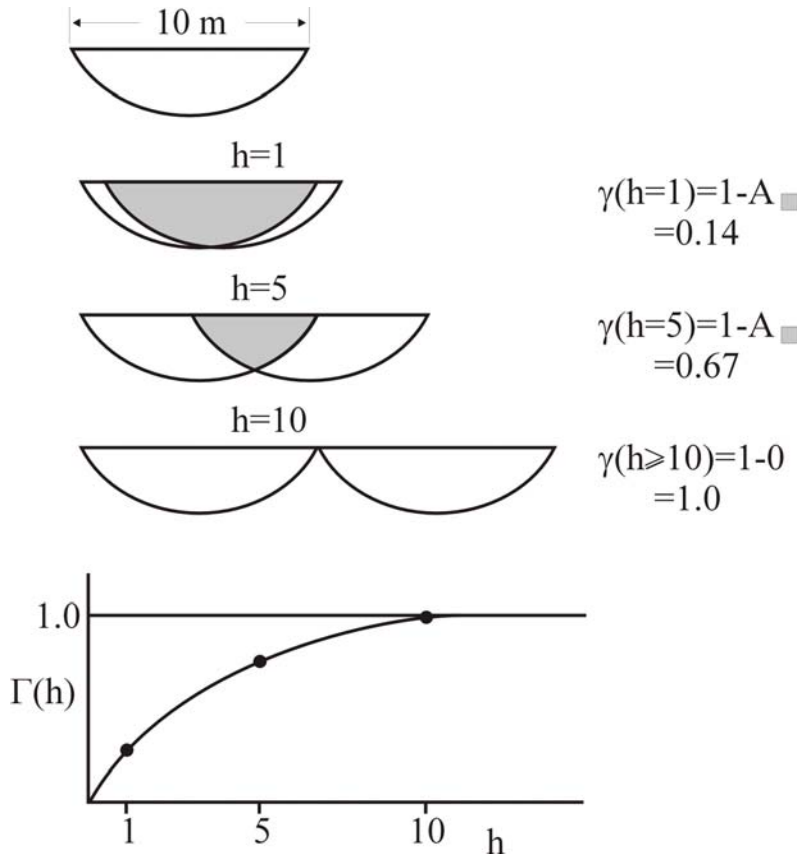

Figure 2

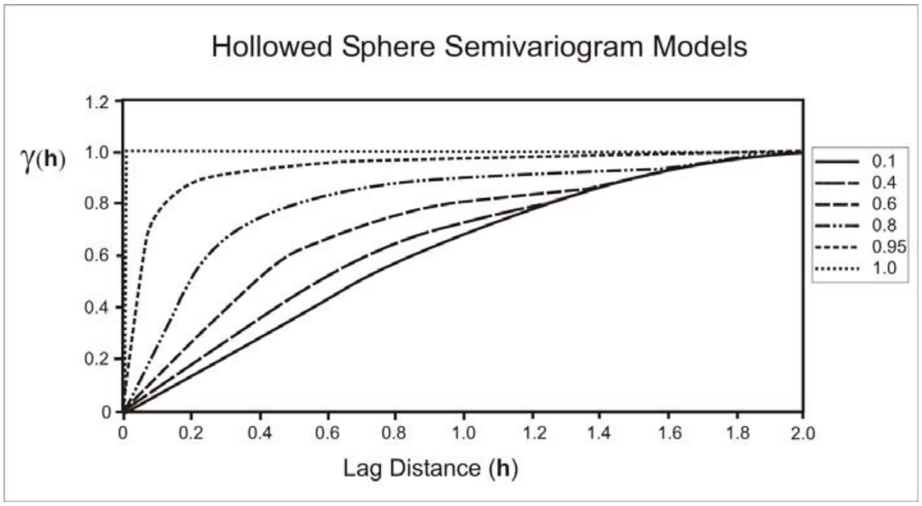

Hollowed Sphere Semivariogram Models
γ(h)
1.2
1.0
0.8
0.6
0.4
0.2
0
0
0.2
0.4
0.6
0.8
1.0
1.2
1.4
1.6
1.8
2.0
Lag Distance (h)
0.1
0.4
0.6
0.8
0.95
1.0

Figure 3

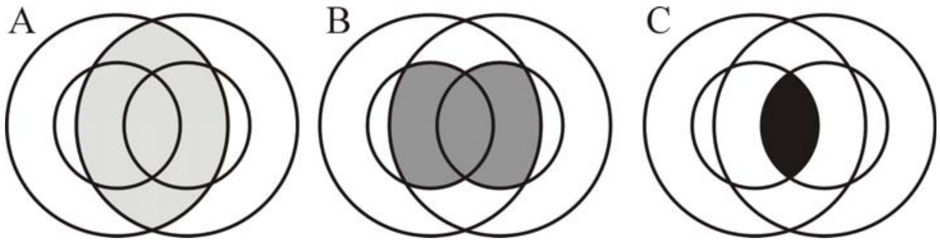

Figure 4

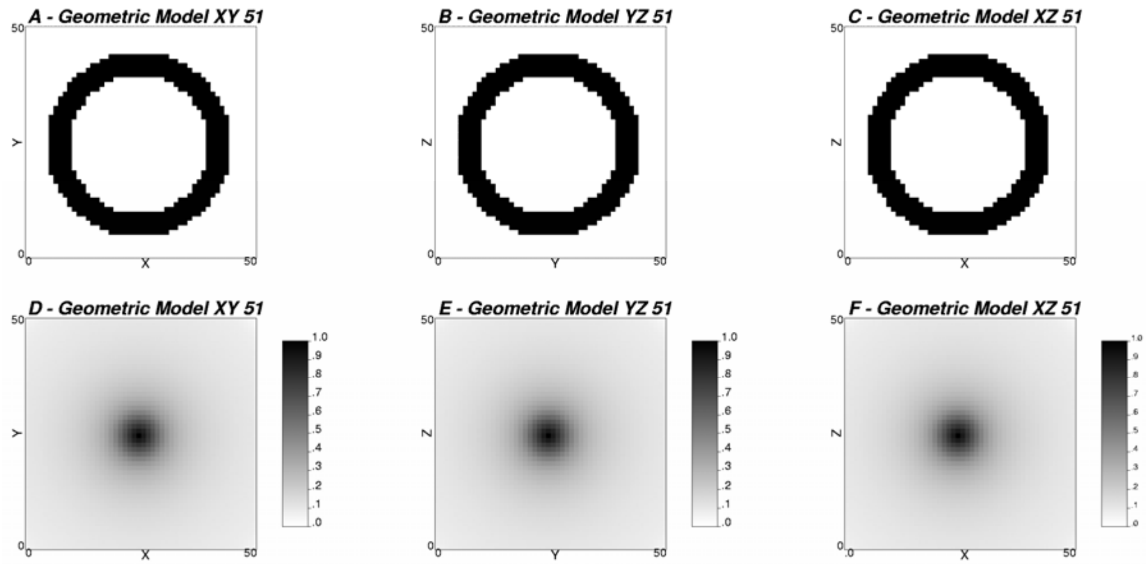

A - Geometric Model XY 51
B - Geometric Model YZ 51
C - Geometric Model XZ 51
D - Geometric Model XY 51
E - Geometric Model YZ 51
F - Geometric Model XZ 51

Figure 5

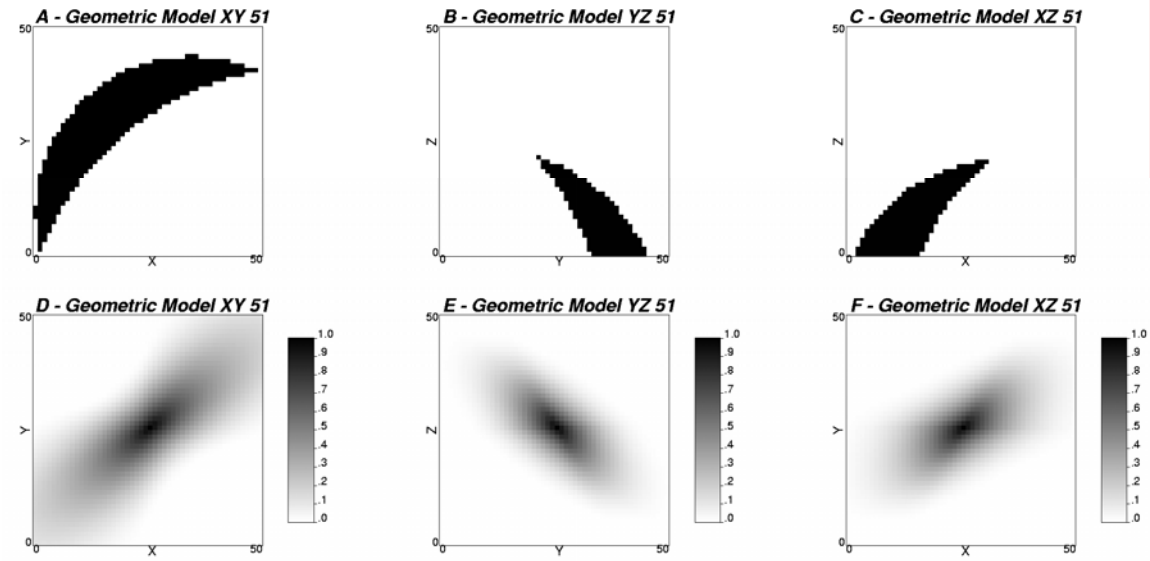
A - Geometric Model XY 51
B - Geometric Model YZ 51
C - Geometric Model XZ 51
D - Geometric Model XY 51
E - Geometric Model YZ 51
F - Geometric Model XZ 51

Figure 6

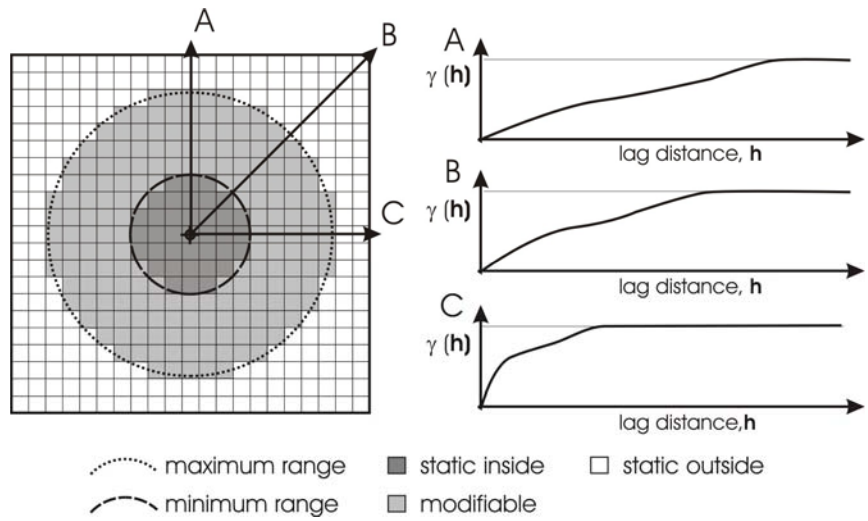
A
B
C
A
γ (h)
lag distance, h
B
γ (h)
lag distance, h
C
γ (h)
lag distance,h
maximum range
minimum range
static inside
modifiable
static outside

Figure 7

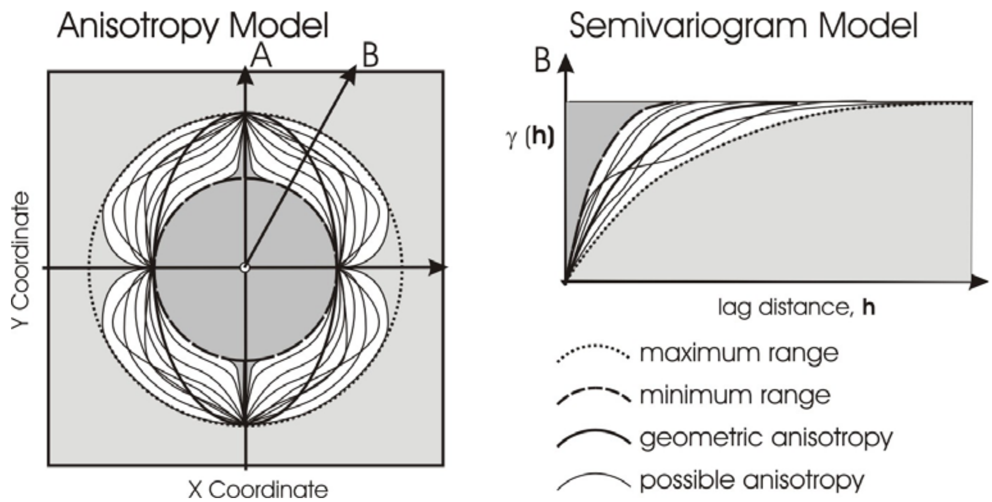

Anisotropy Model
A
B
Y Coordinate
X Coordinate
Semivariogram Model
B
γ (h)
lag distance, h
maximum range
minimum range
geometric anisotropy
possible anisotropy

Figure 8

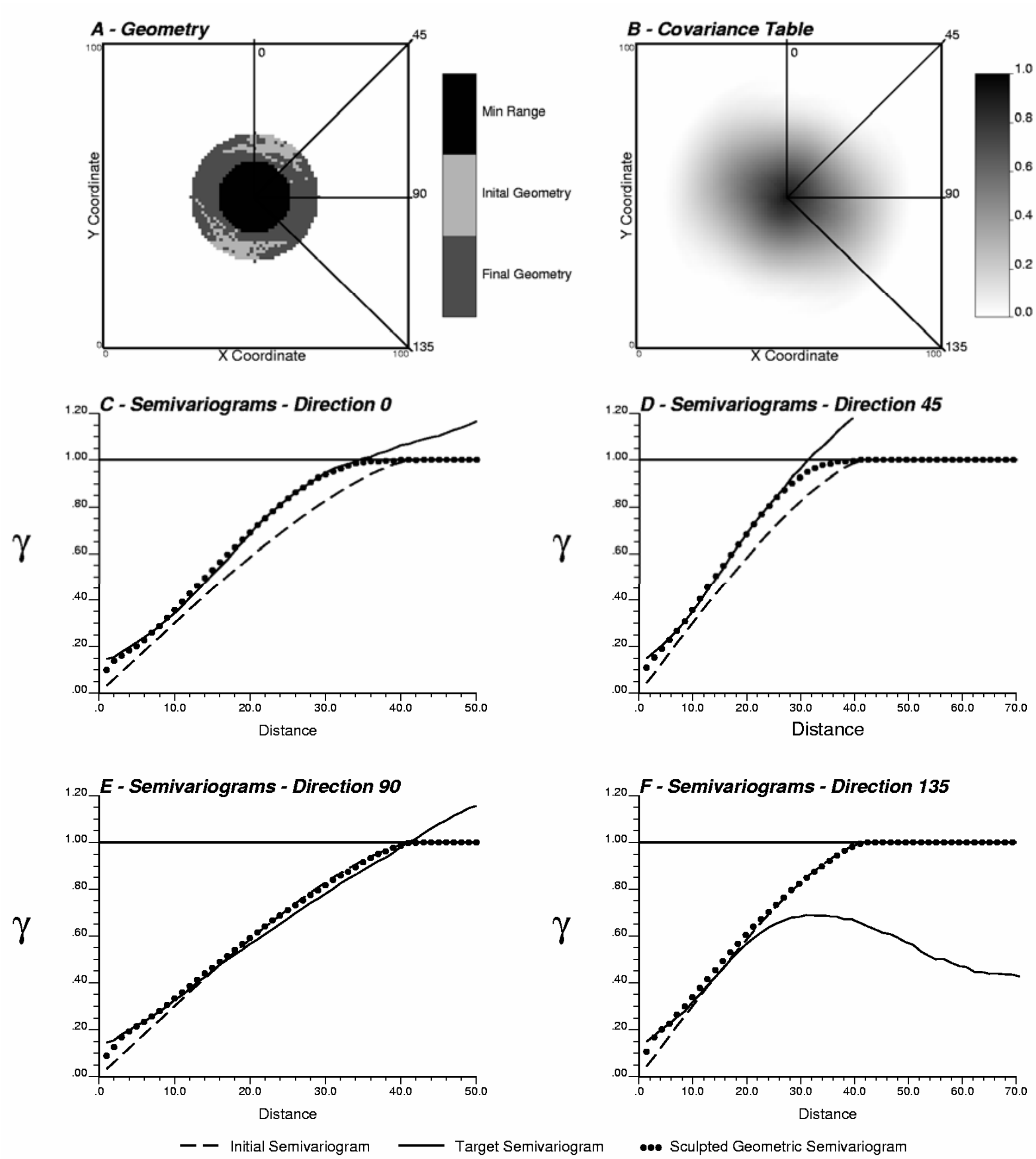
A - Geometry
B - Covariance Table
Min Range
Inital Geometry
Final Geometry
Y Coordinate
X Coordinate
C - Semivariograms - Direction 0
D - Semivariograms - Direction 45
E - Semivariograms - Direction 90
F - Semivariograms - Direction 135
Distance
Initial Semivariogram
Target Semivariogram
Sculpted Geometric Semivariogram

Figure 9

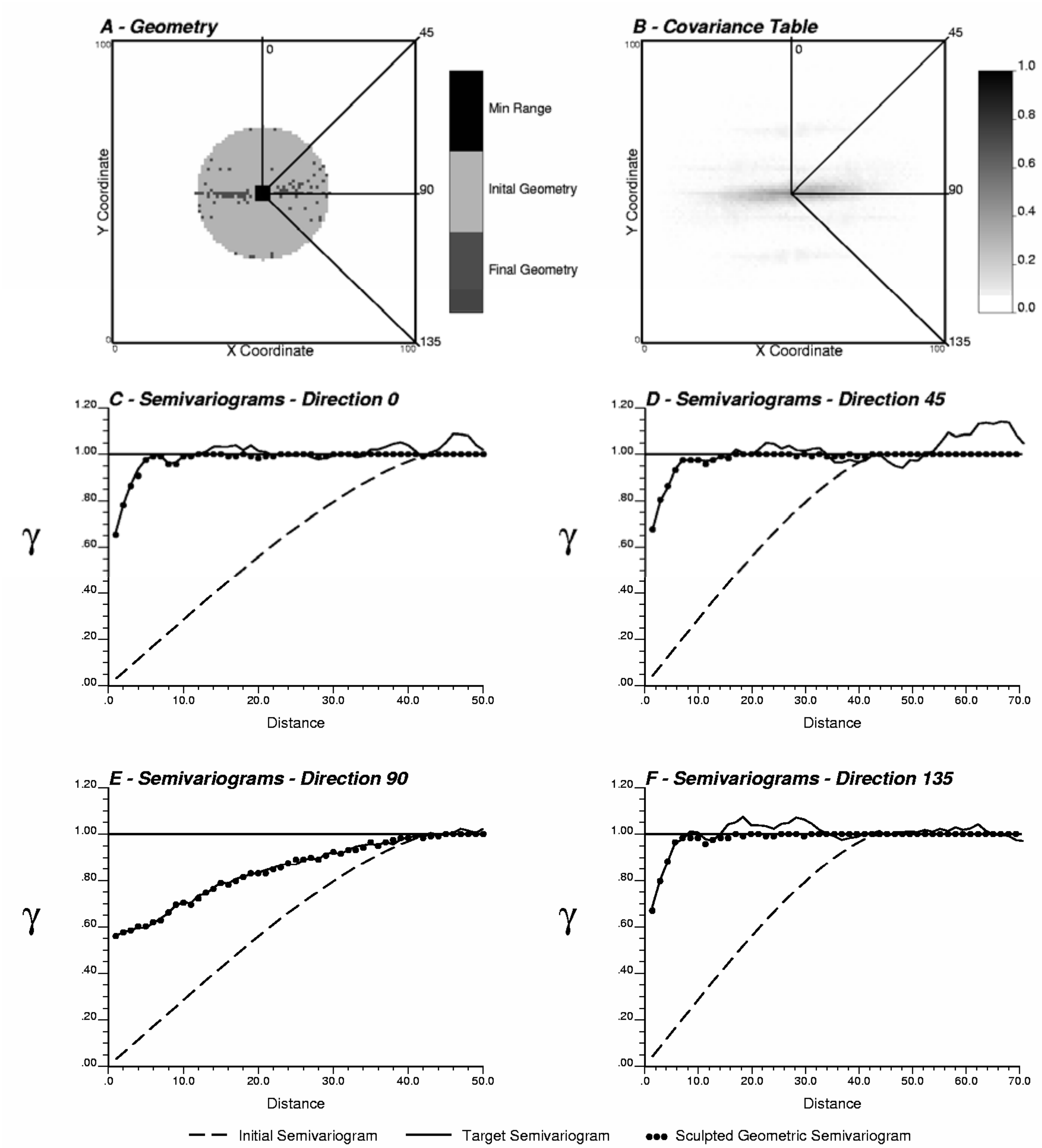
A - Geometry
Min Range
Inital Geometry
Final Geometry
Y Coordinate
X Coordinate
B - Covariance Table
C - Semivariograms - Direction 0
D - Semivariograms - Direction 45
E - Semivariograms - Direction 90
F - Semivariograms - Direction 135
Distance
Initial Semivariogram
Target Semivariogram
Sculpted Geometric Semivariogram

Figure 10